Mechanistic Insights into the DyPB from *Rhodococcus jostii* RHA1 via Kinetic Characterization

Ruben Shrestha[§], Kaimin Jia[§], Samiksha Khadka[§], Lindsay D. Eltis[¶], and Ping Li^{§*}

§Department of Chemistry, Kansas State University, Manhattan, KS 66506, USA

Department of Microbiology and Immunology, The University of British Columbia, 2350 Health Sciences Mall, Vancouver, British Columbia V6T 1Z3, Canada

KEYWORDS: heme peroxidase, steady- and transient-state kinetics, solvent KIE, pH-rate profile, compound I formation and reduction.

ABSTRACT: Dye-decolorizing peroxidases (DyPs) comprise a recently discovered family of heme peroxidases with considerable biotechnological potential. However, the roles of the distal aspartate and arginine in catalysis remain underexplored. Here we elucidated their roles in DyPB from *Rhodococcus jostii* RHA1 using steady- and transient-state kinetics, pH-rate relationship, viscosity, and solvent kinetic isotope effect (sKIE). Consistent with previous data, substitution of the distal aspartate reduced the rate of compound (Cpd) I formation much less dramatically than substitution of the distal arginine. Inspection of the structural data suggests this may be because the distal aspartate is much farther away from the solvent ligand in DyPB than in other B-class DyPs. Replacement of the distal aspartate decreased the rate of Cpd I reduction with ABTS by ~11-fold. An observed inverse sKIE of 0.13 for the WT (k_{cal}/K_M)^{ABTS} is consistent with three waters dissociating from the heme iron during a catalytic cycle, indicating mechanistic importance of aquo release in DyP-catalyzed reactions. An inverse sKIE of 0.25 for Cpd I reduction along with other observations implied that Cpd I is likely in a "wet" form and may undergo two successive $1e^-$ -reduction via an undetected Cpd II. The viscosity effect, sKIE and pH-rate profiles of Cpd I formation demonstrated that, while Cpd 0 deprotonation is likely rate-limiting, O–O scission plays a more significant role in DyPB than in other B-class enzymes. It is further proposed that a rate-limiting conformational change precedes the step that returns the enzyme to its resting state in ABTS oxidation. By highlighting mechanistic differences between similar DyPs, this study provides insight into an important class of enzymes.

Introduction

Dye-decolorizing peroxidases (DyPs) comprise a recently discovered family of heme enzymes that catalyze H₂O₂dependent oxidation of dye substrates, specifically anthraguinone-derived dyes with high redox potentials. 1-4 DyPs have attracted much interest due to their biotechnological potential, including delignification of biomass and degradation of phenolic lignin. 5-14 Based on their primary sequences, DyPs have been classified into four subfamilies: A to D.4, 15 The sequence identity between subfamilies is less than 15%. 1,4 Both A- and B-class DyPs occur exclusively in bacteria, 4, 15 and several act on phenolic lignin model compounds.^{5, 9, 12-13} Recombinant DyPB from Rhodococcus jostii RHA1 can transform Kraft lignin and break down wheat straw lignocellulose in the presence of Mn²⁺.⁵ Intriguingly, expression of the dypB gene in tobacco facilitated subsequent delignification of the biomass and depolymerization of the phenolic lignin.¹⁶

DyPs are distinct from well-known heme peroxidases such as fungal peroxidases (*e.g.* LiP) and horseradish peroxidase in structural fold, substrate specificity, and pH optimum.¹⁻⁴ Furthermore, unlike classical heme peroxidases that use a distal histidine and arginine to perform catalytic functions, ¹⁷⁻¹⁸ DyPs employ an aspartate in place of the distal histidine to accomplish H₂O₂ reduction and enzyme activation.¹⁻⁴ This difference has significant ramifications for the enzyme's properties and its molecular mechanism. For example, we

recently demonstrated that the distal aspartate of *EI*DyP, a B-class DyP from *Enterobacter lignolyticus*, is involved in the formation and reduction of Cpd I and contributes to the enzyme's higher activity at acidic pH.¹⁹ Based on this and similar studies for other classes of DyPs,^{9, 19-22} it has been proposed that the distal aspartate is essential for DyP activity. However, this is contradicted by the studies of A-class DyPs from *Bacillus subtilis* (*Bs*DyP) and *Escherichia coli* O157 (EfeB/YcdB) as well as the B-class DyPs from *R. jostii* RHA1 (DyPB) and *Pseudomonas putida* MET94 (*Pp*DyP), in which substitution of the distal aspartate had an unexpectedly small effect on the respective peroxidase activities of these enzymes.²³⁻²⁶ Given the biotechnological potential of DyPs,⁵⁻¹⁴ we investigated the catalytic roles of distal aspartate and arginine in greater depth.

Using the WT and variant DyPBs from RHA1, the roles of the distal aspartate and arginine were evaluated using steady-and transient-state kinetics together with the studies of the effects of pH, viscosity, and deuterated solvent on the rates. Based on our results, we propose that DyPB utilizes a bisubstrate ping-pong mechanism (Scheme 1) that involves two $1e^-$ -reduction of compound (Cpd) I to an isoform of enzyme resting state (ERS*) via an undetected Cpd II. Subsequently, the ERS* undergoes a conformational change prior to its return to ERS, which was predicted to be rate-limiting for the overall reaction of 2,2'-azino-bis(3-ethylbenzothiazoline-6-sulphonic acid) (ABTS) oxidation. Our study has demonstrated that both

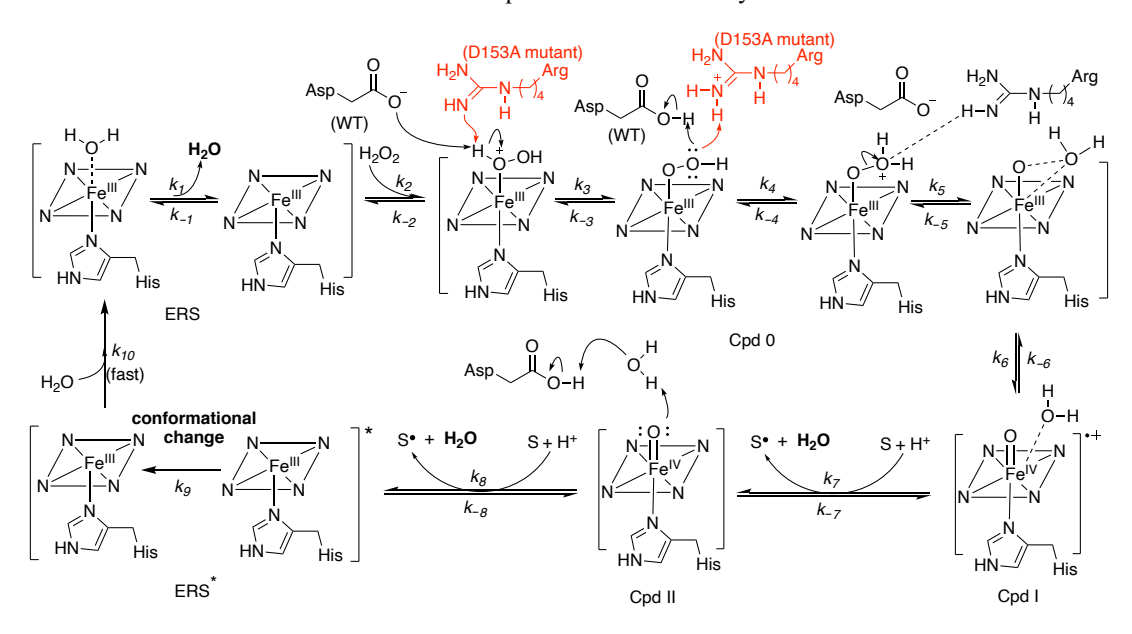


Table 1. Steady-state kinetic parameters of WT and variant DyPBs*

Enzyme		$k_{cat}(s^{-1})$	$K_M(\mu M)$		$k_{cat}/K_M({ m s}^{-1}{ m M}^{-1})$	
(pH optimum)			ABTS	H_2O_2	ABTS	H_2O_2
WT	In H ₂ O	(3.22±0.16)×10 ²	(6.50±0.97)×10 ²	$(2.86\pm0.29)\times10^3$	(4.95±0.98)×10 ⁵	(1.14±0.06)×10 ⁵
(3.5)	In D ₂ O	$(3.06\pm0.11)\times10^2$	(8.08±0.59)×10	$(2.45\pm0.25)\times10^3$	(3.79±0.12)×10 ⁶	$(1.26\pm0.03)\times10^5$
	sKIE	1.08±0.05			0.13±0.02	0.92±0.07
D153A (5.0)		(4.71±0.03)×10	$(1.40\pm0.22)\times10^3$	$(6.89\pm0.94)\times10^{2}$	(3.36±0.36)×10 ⁴	$(6.78\pm0.60)\times10^4$
D153	3E (3.5)	$(2.30\pm0.07)\times10^{2}$	$(3.43\pm0.38)\times10^{2}$	$(1.84\pm0.09)\times10^3$	(6.70±0.76)×10 ⁵	$(1.40\pm0.02)\times10^5$
D153H (4.0)		(7.27±0.10)×10	$(1.43\pm0.65)\times10^3$	$(2.29\pm0.16)\times10^3$	$(5.08\pm0.98)\times10^4$	$(3.31\pm0.04)\times10^4$
D153N (4.0)		(4.20±0.42)×10	$(3.18\pm1.81)\times10^2$	$(6.87\pm0.45)\times10^3$	$(1.32\pm0.55)\times10^5$	$(5.39\pm0.10)\times10^3$
R244L (5.0)		(2.31±0.03)×10	$(1.23\pm0.65)\times10^3$	$(1.83\pm0.27)\times10^4$	$(1.88\pm0.40)\times10^4$	$(1.37\pm0.21)\times10^3$

^{*}Assays were performed at enzymes' respective pH optima (Table S2).

distal residues are catalytically important in DyPB. However, substitution of the distal aspartate had a much lesser effect on the rate of Cpd I formation than the distal arginine, which could be rationalized by their respective distances to the sixth water ligand of heme iron in the ERS. In addition, deprotonation of Cpd 0 was proposed to be a rate-determining step (RDS) in Cpd I formation, though the O–O scission appeared to play a more significant role in DyPB than in other B-class enzymes. The significant inverse solvent kinetic isotope effects (sKIEs) associated with DyPB suggested that aquo release is mechanistically important. The implications of these findings are discussed with respect to other DyPs.

Results

Steady-state kinetics of DyPBs. To investigate the importance of the distal aspartate in catalysis, variants were generated by site-directed mutagenesis (Table S1) and purified by affinity chromatography (Figure S1-A). We determined kinetic parameters of each of the aspartate variants at their respective pH optima (Figures S2-A/B and Table S2). As summarized in Tables 1 and S3 and depicted in Figure 1, substituting Asp153 with alanine resulted in \sim 85% loss of activity (k_{cat}) toward ABTS and \sim 50% loss toward Reactive Blue 19 (RB19). This

substitution also doubled the K_M value for ABTS and decreased the $(k_{cat}/K_M)^{ABTS}$ value ~15-fold. Since the same substitution enhanced the H_2O_2 binding affinity by ~4-fold, the decrease in

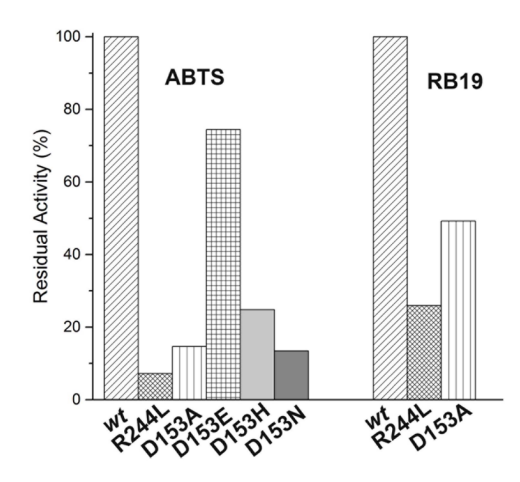


Figure 1. Residual activities of WT and variant DyPBs with ABTS and RB19 in the presence of H_2O_2 at enzyme-saturating concentrations. Conditions of enzyme assays are described in Table S2.

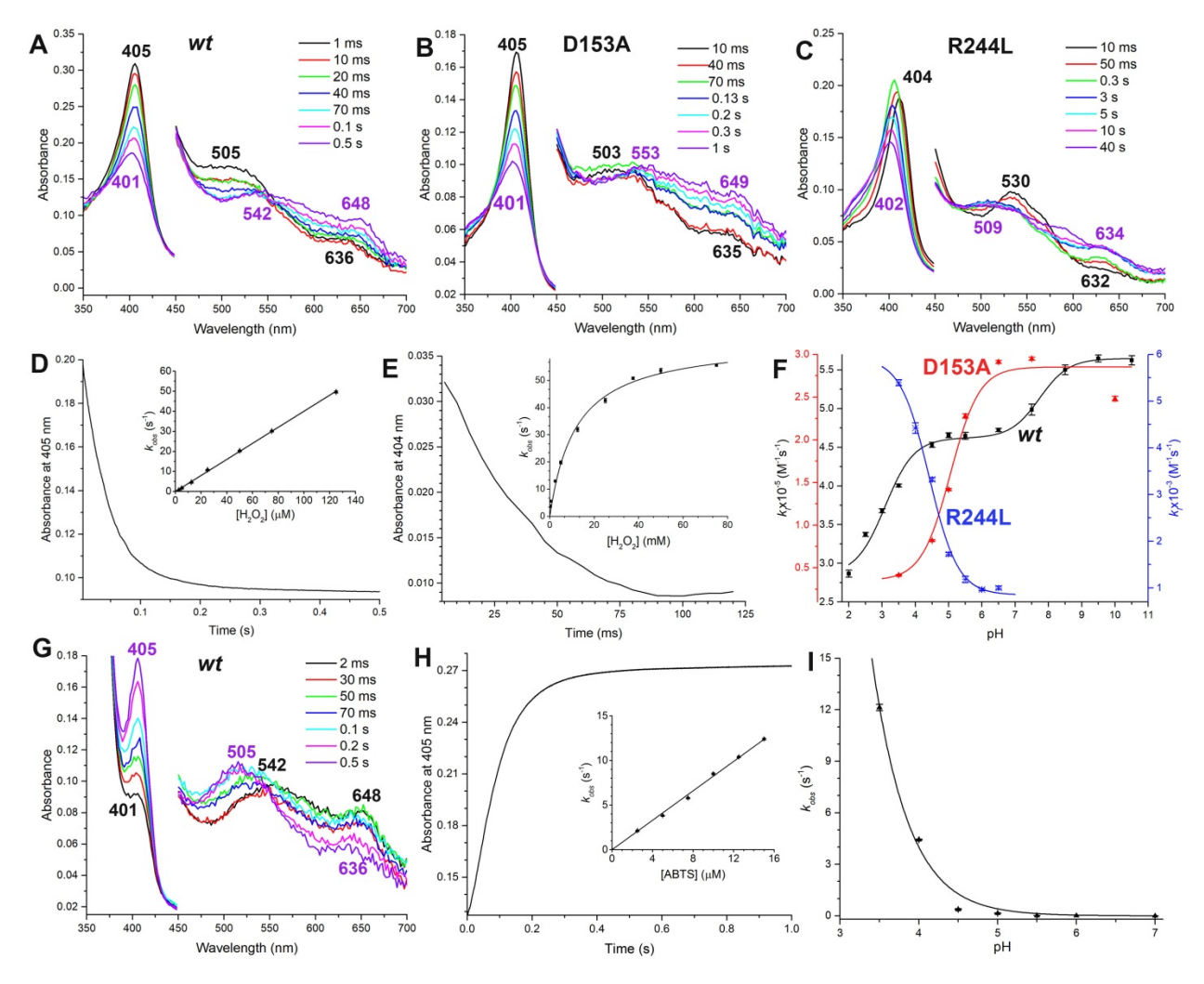


Figure 2. Transient-state kinetics of DyPB-catalyzed reactions. Spectra recorded at 450-700 nm are magnified 4 times. Reactions were performed at the variants' respective optimal pH (see Table 2). (A–C) Spectral transitions of Cpd I formation between enzymes and H_2O_2 at final concentrations of 2.5 and 50 μM, respectively. Enzymes used are the WT (A), D153A (B), and R244L (C). (D–E) Formation of Cpd I monitored at the Soret bands for the WT (D) and R244L (E). Insets represent determination of the second-order rate constant of Cpd I formation. (F) pH-dependence of the second-order rate constants of Cpd I formation for the WT (black), D153A (red), and R244L (blue). The color of Y-axis and curves correspond to each other. (G) Spectral transitions of 2.5 μM WT Cpd I reduced by 10 μM ABTS in the presence of 100 μM ascorbate at pH 3.5. Cpd I was produced by reacting 2.5 μM WT with 2.5 μM H_2O_2 at pH 3.5 followed by a 10-s delay. (H) Regeneration of ERS at pH 3.5 from the WT Cpd I in the presence of ABTS and ascorbate monitored at 405 nm. The inset represents determination of the second-order rate constant of Cpd I reduction. (I) pH-dependence of 2.5 μM WT Cpd I reduced with 15 μM ABTS at various pH in the presence of 150 μM ascorbate.

 $(k_{cat}/K_M)^{\text{H}_2\text{O}_2}$ was much lesser (~2-fold). Among the aspartate variants, D153E had the highest activity, retaining ~72% WT activity toward ABTS. This is consistent with the conservative nature of the substitution: the only difference between aspartate and glutamate is an extra methylene group, which might introduce steric hindrance. Replacement of Asp153 with asparagine resulted in ~87% decrease in activity with ABTS, likely due to disruption of hydrogen bonds involving the carboxylate group. Since fungal lignolytic enzymes such as LiP have a distal histidine, $^{27-28}$ the D153H variant was constructed. This variant had ~23% of the WT's activity toward ABTS. Overall, these results demonstrated that the distal aspartate in DyPB contributes significantly to catalysis.

To elucidate the importance of the distal Arg244, it was replaced with a leucine, resulting in a 93% decrease in the k_{cat} for ABTS. The catalytic efficiencies (k_{cat}/K_M) for ABTS and H_2O_2 were ~26- and ~83-fold lesser relative to the WT,

respectively. While the k_{cat} of the variant with RB19 dropped by ~74%, so did its K_M value, and its catalytic efficiency stayed almost the same as the WT. By contrast, the K_M value of the R244L variant for H₂O₂ was ~5-fold higher than that of the WT, and the $(k_{cat}/K_M)^{\text{H}_2\text{O}_2}$ value was ~16-fold lesser. Overall, these results support the previous findings that the distal arginine contributes more to catalysis in DyPB than the distal aspartate.²⁵

Transient-state kinetics of Cpd I formation. As shown in Scheme 1, the catalytic cycle of heme peroxidases generally involves a ferric resting state, ERS, and intermediates consisting of Cpds 0, I, and II, which are key to understanding the enzymes' chemistry and biology. WT and variant DyPBs rapidly formed Cpd I when reacted with H_2O_2 at their respective pH optima. Representative spectral changes are shown in Figures 2A–C and the characteristic absorbance maxima for the ERS and Cpd I are summarized in Table S4. To determine the second-order rate constants of Cpd I formation, k_I , reactions

Table 2. Transient-state kinetic parameters and pK_a of WT and variant DyPBs^{*}

Table 2. Transfellt-state killetic parameters and p_{K_a} of will and variant DyFBs									
Enzyme		Cpd I reduction							
(pH optimum)	pK_a		$k_I (\mathrm{M}^{-1} \mathrm{s}^{-1})$	$k_{ERS} \left(\mathbf{M}^{-1} \mathbf{s}^{-1} \right)$					
	Asp	Arg							
WT (3.5)	3.08±0.11	7.73±0.19	(4.00±0.02)×10 ⁵	(8.24±0.06)×10 ⁵					
D153A (5.0)		5.05±0.16	(1.42±0.02)×10 ⁵	(7.38±0.08)×10 ⁴					
D153E (3.5)	N.A.	N.A.	(2.46±0.04)×10 ⁵	N.A.					
D153H (4.0)	N.A.	N.A.	(1.60±0.02)×10 ⁴	N.A.					
D153N (4.0)	N.A.	N.A.	$(7.14\pm0.18)\times10^3$	N.A.					
R244L (5.0)	4.41±0.07		$(1.72\pm0.03)\times10^3$	N.D.					

^{*}Assays were performed at enzymes' respective pH optima (Table S2); N.A.: not available; N.D.: not detected

were followed by disappearance of the Soret band of each enzyme's ERS at its λ_{max} (Figures 2D-2E). Single-exponential decays were fitted to the resulting traces to obtain k_{obs} , which was then plotted against $[H_2O_2]$ to derive k_I (insets in Figures 2D-E). While the WT and D153A yielded linear plots from which k_I values could be calculated, the R244L variant gave saturation kinetics, suggesting presence of a preequilibrium (K_D) between the R244L and H_2O_2 prior to Cpd I formation (k)(Eq. 1 in SI). Accordingly, k_I values of the WT and D153A were calculated from the slopes of the linear curves, and the k_I value for R244L was determined from k/K_D using Eq. 2 in SI. Table 2 summarizes the k_I values determined at enzymes' respective pH optima. For the WT, the k_I was also determined at 648 nm (Figure S3), where Cpd I formation and decay could be monitored. The value derived from 648 nm was $(4.16\pm0.03)\times10^5$ M⁻¹s⁻¹, in agreement with the k_I determined at 405 nm (Table 2). Consistent with the previous report, 30 the WT Cpd I was remarkably stable at pH 3.5 with a half-life time of \sim 32 min when it was generated using a 20 molar excess of H_2O_2 .

Consistent with the previous report,²⁵ the distal arginine was found to be much more important than the distal aspartate in DyPB Cpd I formation. At their respective pH optima, the R244L formed Cpd I at 0.4% the rate of the WT. By contrast, the most impaired aspartate variant, D153N, retained 1.8% k_I of the WT. Interestingly, the k_I values of the D153A and D153H were found to be 35% and 4% that of the WT, respectively, even though the latter was expected to be more reactive due to its resemblance to the classical plant peroxidases. This discrepancy may be due to significant changes in the heme environment, which are further suggested by the bathochromic shift of the heme's absorption maxima in D153H (Figure S1-B). The discrepancy may also be explained from their crystal structures discussed below. Finally, the k_I values are consistent with the $(k_{cat}/K_M)^{\text{H}_2\text{O}_2}$ obtained from the steady-state kinetics.

pH-dependence of Cpd I formation. Determination of reaction rates as a function of pH can provide critical information about enzyme mechanism.³¹ These rates are sensitive to the pK_a values of catalytically important residues, a value that can be influenced by the enzymes' environment.³¹ Accordingly, we investigated the pH-dependence of Cpd I formation (k_I) in the WT and variant DyPBs. Equations 3–5 in SI were fitted to plots of k_I vs pH.³² Similar to B-class EIDyP,¹⁹ the rate of Cpd I formation in the WT increased with pH. The curve (Figure 2F) had two inflection points, at 3.08 and 7.73 (Table 2), which were assigned to Asp153 and Arg244, respectively. To examine whether this assignment was correct, we also determined the pH-rate profiles of D153A and R244L.

Consistent with our prediction, each mutant only had a single inflection point (Figure 2F). Furthermore, similar to the WT, the rate of Cpd I formation in D153A increased as pH increased. However, the trend in R244L was the opposite: the rate decreased with increasing pH. Finally, the pK_a assigned to Asp153 is close to the intrinsic pK_a of aspartate, 3.65. By contrast, that assigned to Arg244 is 4.75 pK_a units lower than the intrinsic value of arginine, 12.48. Indeed, this shift is greater than the 3.80 pK_a unit shift observed for the distal arginine of the EIDyP, ¹⁹ highlighting the difference in their respective heme environment.

Transient-state kinetics of Cpd I reduction. The reduction of Cpd I was investigated using a sequential-mixing mode. Cpd I was generated by mixing the enzyme with 1 equiv. H₂O₂. After a 10-second delay to maximize Cpd I formation, the mixture was then rapidly mixed with ABTS in the presence of ascorbate. Ascorbate was used of to quench the ABTS radical, eliminating its spectral interference in the Soret band region.³³ This allowed us to use low concentrations of ABTS to maintain pseudo-firstorder reaction conditions.³³ A typical spectral transition is shown in Figure 2G, where band characteristics of Cpd II were not detected. Therefore, the rate of Cpd I reduction was indirectly determined at pH 3.5 at 405 nm corresponding to ERS generation (Figure 2H). The second-order rate constant (k_{ERS} , inset in Figure 2H), calculated after correcting for reduction by ascorbate, was ~2 times faster than the rate of Cpd I formation at pH 3.5 (Table 2).

We also investigated the pH-dependence of Cpd I reduction (k_{ERS}) by ABTS. No reduction was observed above pH 5.0. Furthermore, the instability of DyPB precluded the rate determination below pH 3.5. As shown in Figure 2I, the rate increases drastically as the pH decreases, indicating that acidic conditions favor Cpd I reduction. Fitting the equation used previously ¹⁹ to the data gave a pK_a of 2.28, suggesting an ionizable acidic residue, possibly Asp153, participates in this reduction process. Replacement of Asp153 with alanine reduced the reduction rate by 11-fold compared to the WT (Table 2).

Viscosity effects on steady- and transient-state kinetics. D_2O is ~25% more viscous than H_2O at room temperature ³⁴ and this viscosity could mask intrinsic sKIEs. ³⁵ Therefore, sucrose was employed as a viscosogen to probe the viscosity effects on steady- and transient-state kinetics. Results are shown in Figures 3A and S4 and summarized in Table 3. In these plots, a slope of 1 indicates a completely diffusion-controlled reactions, while diffusion-independent reactions have a slope of zero. For the WT, k_{cat} was diffusion-independent. By contrast,

 $(k_{cat}/K_M)^{\rm ABTS}$ was determined to be 60% diffusion-controlled. Inverse viscosity effects were observed for the $(k_{cat}/K_M)^{\rm H_2O_2}$ and k_I , for which the averages were 0.98 and 0.88, respectively, at a relative viscosity ($\eta_{\rm rel}$) of 1.25. These results suggest that Cpd I reduction by ABTS is diffusion-dependent. Moreover, it was observed that the viscosity effect on Cpd I formation (k_I) is pH independent for the WT and variant DyPBs.

An inverse viscosity effect was observed for the k_I of D153A, with an average of 0.68 at $\eta_{\rm rel} = 1.25$ (Table 3 and Figure S4-A). The k_I of R244L, calculated from k/K_D , showed no significant viscosity effect (Table 3 and Figure S4-B). It is of note that inverse viscosity effects have been reported for several unrelated enzymes, 35-38 although the cause for this and the corresponding mechanistic implications remain unknown. Nevertheless, effects on enzyme activities resulting from changes in solvent viscosity have to be considered when interpreting sKIEs. For example, if there is an inverse viscosity effect arising from the more viscous D2O, the intrinsic sKIE will be underestimated for an observed normal sKIE and overestimated for an observed inverse sKIE.

Solvent kinetic isotope effects (sKIEs) of steady- and transient-state kinetics. The sKIE is a useful mechanistic probe of reactions involving solvent-exchangeable protons. 19, 39-40 Generally, sKIEs are calculated from pH-independent regions of kinetic parameters in H₂O and D₂O. DyPs have optimal activities at an acidic pH.1-4 Consequently, the pH-independent region for their steady-state kinetics should appear in an acidic region. However, WT DyPB was unstable below pH 3.5. Therefore, the sKIEs of steady-state kinetics were evaluated at pL (= pH/pD) 3.5. None of the k_{cat} or k_{cat}/K_M values (Table 1) exhibited significant sKIEs except for ${}^{D}(k_{cat}/K_{M})^{ABTS}$ $[=^{\text{H}_2\text{O}}(k_{cat}/K_M)^{\text{ABTS}}]$, for which a significant inverse sKIE of 0.13 (Table 1) was determined. Since only a small normal viscosity effect (Figure 3A, 1.19 at $\eta_{rel} = 1.25$) was observed for $(k_{cat}/K_M)^{ABTS}$, it suggests that the intrinsic sKIE of $(k_{cat}/K_M)^{ABTS}$ is close to the observed value of 0.13. The magnitude of this sKIE implies the dissociation of approximate three water molecules from the heme iron as discussed below.

To determine sKIEs of Cpd I formation and reduction, experiments of transient-state kinetics were performed in H₂O and D₂O at various pL. The sKIE was then calculated from pHindependent regions. As shown in Figure 3B and summarized in Table 3, two pH-independent regions were found for the formation of WT Cpd I, giving two small normal sKIEs of 1.07 and 1.22. The corresponding intrinsic sKIEs should be larger than the observed, as both regions displayed an inverse viscosity effect of 0.88. The D153A exhibited an observed inverse sKIE of 0.55 at its pH-independent region (Table 2 and Figure S4-A), which was attributed mainly to the viscosity difference between D₂O and H₂O. Thus, the intrinsic sKIE of D153A Cpd I formation should be ~1. Since no viscosity effect was identified for the R244L, the observed sKIE of 0.92 (Table 2 and Figure S4-B) should be close to the intrinsic value. Proton inventories were not performed, as these enzymes did not display significant intrinsic sKIEs of Cpd I formation.

Based on the pH-rate profile of the WT Cpd I reduction (Figure 2I), its pH-independent region is at or below pH 3.5. However, the enzyme is unstable below pH 3.5. Consequently, the sKIE of Cpd I reduction was determined in H₂O and D₂O at pL 3.5, giving a significant inverse sKIE of 0.25 (Figure 3C). A similar inverse sKIE of 0.32 was also obtained for the D153A Cpd I reduction at pL 5.0. Since a small normal viscosity effect was predicted for Cpd I reduction [based on the observed

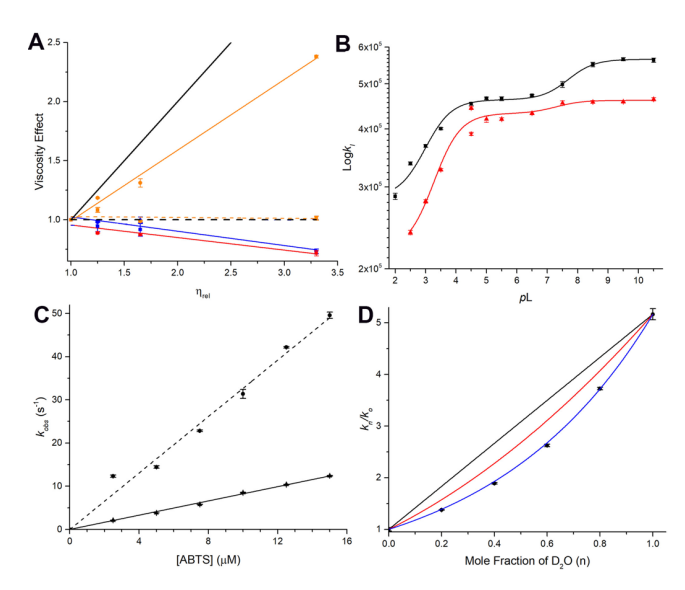


Figure 3. Viscosity effects and sKIEs of WT DyPB. (A) Viscosity effects of $(k_{cat})^{\rm ABTS}$ (yellow dash), $(k_{cat}/K_M)^{\rm ABTS}$ (yellow solid), $(k_{cat}/K_M)^{\rm H2O_2}$ (blue solid), and $k_I{}^I$ (red). The black solid and dash lines represent completely diffusion-controlled and diffusion-independent reactions, respectively. All experiments were performed at pH 3.5. (B) Rates of the Cpd I formation at various pL in H2O (black) and D2O (red). (C) Rates of the Cpd I reduction with ABTS in the presence of ascorbate at pH 3.5 in H2O (solid) and D2O (dash). (D) Proton inventory of the Cpd I reduction with ABTS. The black dots represent experimental data. The black, red, and blue lines represent simulations of involving one [eq. $\frac{k_n}{k_0} = (1-n+\frac{n}{0.1936})^2$], and many protons [eq. $\frac{k_n}{k_0} = (\frac{1}{0.1936})^n$], respectively.

Table 3. Effects of viscosity (η) and solvent isotope (sKIE) on transient-state kinetics

transferr state mineres								
Enzyme	η on k_I	s KIE of k_I	s KIE of k_{ERS}					
WT	WT 0.88±0.01 1.07±0.02 and 1.22±0.01		0.25±0.01					
D153A	0.68±0.01	0.55±0.01	0.32±0.04					
R244L 1.01±0.03		0.92±0.01	N.D.*					

*N.D.: not detected.

viscosity effect of 1.19 at $\eta_{\rm rel} = 1.25$ for $(k_{cal}/K_M)^{\rm ABTS}$], the corresponding intrinsic sKIEs should be close to what was measured, suggesting dissociation of two water molecules from the metal center during Cpd I reduction.

This is consistent with the *s*KIE of steady-state kinetics and further demonstrates that aquo release is mechanistically important for DyPB-catalyzed oxidation. Moreover, since only one water is produced during Cpd I reduction, the inference that two water molecules are released implies that one is bound to Cpd I prior to its reduction (*i.e.* Cpd I is hydrated and in a "wet" form). A proton inventory of the WT Cpd I reduction displays a concave curvature (Figure 3D), implying an inverse *s*KIE and transfer of more than one proton in the RDS.⁴¹ The data obtained were best described by the Gross-Butler Eq. 6 shown in SI involving simultaneous transfer of many protons, that is, $k_n/k_o = (1/0.19)^{n}$.⁴² This is also reflected in Scheme 1, where production of the water molecule from Cpd I reduction uses a distal aspartate, one or more bridging water molecules, and a proton.

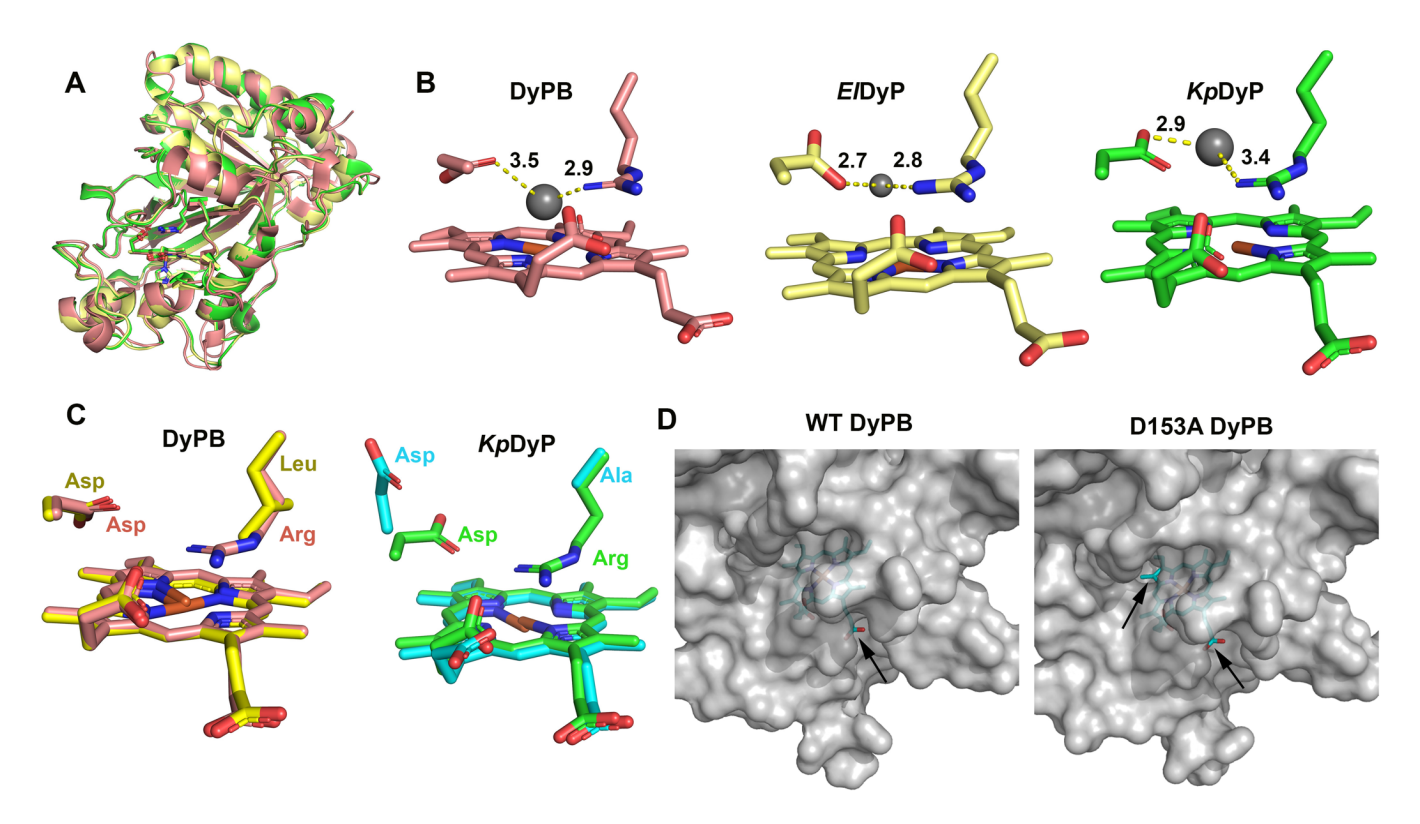


Figure 4. Structural comparisons of B-class DyPs. (A) Overlay of the WT DyPB (pink, PDB 3QNS), EDyP (yellow, PDB 5VJ0, RMSD = 0.872 Å with DyPB), and EPDyP (green, PDB 6FKS, RMSD = 0.908 Å with DyPB). The heme and catalytic residues are shown as sticks. (B) Heme distal sides of the WT DyPB, EDyP, and EPDyP. Distances of the distal residues to the sixth water ligand (represented by a grey sphere) are shown. (C) Overlay of the heme pockets for DyPB [WT (pink) and R244L (bright yellow, PDB 3VEG)] and EPDyP [WT (green) and R232L (cyan, PDB 6FKT)]. (D) The shallow heme accessing channels in the WT DyPB and its D153A variant (PDB 3VEC). Protein surfaces are colored in grey and arrows indicate the access channels.

Discussion

Relative catalytic importance of the distal residues. Our present studies have shown that the distal aspartate contributes to catalysis in DyPB. However, it contributes less than the distal arginine. This contrasts to what has been found in the B-class ElDyP and VcDyP from Vibrio cholera, in which the distal aspartate is of greater catalytic importance than the distal arginine. 19, 22 Nevertheless, it is unclear to what extent this is true in other A- and B-class DyPs. For example, the distal aspartate was claimed to be nonessential for the catalytic activity of A-class BsDyP and B-class PpDyP. 23-24 Such claims need to be reevaluated as the enzymes were inhibited by low μ M concentrations of H₂O₂, ²³⁻²⁴ preventing determination of their steady-state kinetic parameters with ABTS at saturating concentrations of H₂O₂. Further, the kinetic parameters of BsDyP were determined using proteins with partial heme occupancy.²⁴ The claim is further confounded by our finding that the contribution of the distal aspartate in catalysis in DyPB is dependent on the identity of the reducing substrate (Figure 1 and Table 1), suggesting existence of different modes of oxidation for different substrates in DyPs. 43 Finally, transientstate kinetics indicate that the distal aspartate in DyPB plays a more significant role in Cpd I reduction than in Cpd I formation. Given the complexity of the distal aspartate, investigating its role in other A- and B-class DyPs is warranted.

The distal arginine has been reported to be essential for all DyPs except for BsDyP.²⁴ As noted above, steady-state kinetics of BsDyP are complicated by inhibition by H₂O₂ and incomplete heme occupancy. Nevertheless, as with the distal

aspartate, the role of Arg244 in catalysis is also substrate-dependent because its substitution had a larger effect on the k_{cat} measured with ABTS than with RB19. Moreover, transient-state kinetics revealed that Arg244 plays an indispensable role in Cpd I formation in DyPB. Finally, the UV-Vis spectrum of the R244L variant differed significantly from those of the WT and D153A DyPBs (Figure S1-B), indicating that the distal arginine contributes to the heme microenvironment in a way that the distal aspartate does not. Together, these results suggest that the distal arginine in D153A is likely to participate in protonation and deprotonation of Cpd 0 in the same way as the distal aspartate in the WT (Scheme 1).

Structural regulation of the relative importance of distal residues. Comparison of the structures of DyPB, ElDyP and KpDyP from Klebsiella pneumonia suggests a possible rationale for the relative catalytic importance of the distal aspartate in B-class DyPs. 19, 30, 44 Overall, these structures are superimposable with an RMSD of 0.872-0.908 Å (Figure 4A). Inspection of the enzyme's respective heme pockets (Figure 4B) revealed that the distal aspartates in DyPB, ElDyP and KpDyP are located, respectively, 3.5, 2.7, and 2.9 Å away from the water molecule that acts as the sixth ligand of the heme iron. The distal arginines are positioned 2.9, 2.8, and 3.4 Å away from the water ligand in DyPB, ElDyP and KpDyP, respectively. Since this water is displaced by the H₂O₂ in Cpd I formation, interactions of the solvent ligand with the distal residues likely reflect those present during Cpd I formation. More specifically, a short distance between the distal residue and H₂O₂ is expected to facilitate proton transfer and O-O scission in Cpd I formation (Scheme 1). In this respect, the relative proximity of the distal aspartate to the water ligand is consistent with the more profound catalytic effect of substituting this residue with alanine in EIDyP and KpDyP (\sim 3-4 orders of magnitude reduction in k_I). In contrast, the similar distances between the distal arginine and water ligand in EIDyP and DyPB are consistent with the similar effect of their substitution on Cpd I formation: replacement in either enzyme resulted in an \sim 3 orders of magnitude reduction in k_I .

Although KpDyP has the longest distance of the distal arginine to water ligand (3.4 Å) among the three enzymes discussed here, it still displays a similar reduction of k_I (by ~ 3 orders of magnitude) as the other two, which is unexpected and is mainly attributed to the reorganization of the heme pocket. It has been reported that replacing the distal arginine in KpDyP induces a collapse and reorganization of the heme cavity, leading to the loss of the distal heme access channel.44 Additionally, the distal aspartate undergoes a significant conformational change, resulting in its side chain pointing away from the heme iron in the R232A variant of KpDyP (Figure 4C) and drastic rate reduction of Cpd I formation. A similar detrimental effect on protein structure was not observed with the R244L variant of DyPB, in which the integrity of the heme pocket was retained (Figure 4C).²⁵ These results imply that substitution of the distal arginine in KpDyP would have minimally reduced the rate of Cpd I formation if structural integrity of the heme pocket was maintained. This supports our aforementioned proposal that the relative catalytic importance of the distal residues in B-class DyPs is likely regulated by their distances to the sixth water ligand of the heme iron.

Somewhat unexpectedly, the D153A variant of DyPB was more active than the D153H, forming Cpd I almost 10-time faster. Substitution was expected to mimic the catalytic machinery of plant peroxidases. Inspection of the structures of the WT and D153A revealed the presence of an additional shallow pocket leading to the distal side of the heme in the D153A (Figure 4D). This pocket is much wider than the proposed distal solvent access channel for the H₂O₂ in the WT,³⁰ and may partially compensate for the loss of the distal aspartate in D153A by facilitating the access of H₂O₂ to the heme. However, such compensation is absent from the D153H, resulting in a lower activity than the D153A for Cpd I formation. Interestingly, the steady-state kinetics showed that, for the overall reaction, the k_{cat} of the D153H was still ~1.5 times higher than that of the D153A in ABTS oxidation, which provides additional evidence that the distal aspartate in DyPB is critical for Cpd I reduction, as the function of the aspartate as a general acid can be partially rescued by the histidine, but not alanine.

Mechanistic implications of sKIEs. Detailed analyses were performed for sKIEs along with viscosity effects for transient- and steady-state kinetics. Their mechanistic implications are discussed below from three aspects.

Aquo release in DyPB. Inverse sKIEs are not commonly observed and can have various origins including catalysis involving thiols, medium effects, and the dissociation of water from metal centers.³⁵ DyPB contains three cysteine residues, of which the closest, C116, is 21.7 Å away from the heme iron. Thus, it is unlikely that any of the cysteines participates directly in catalysis. Medium effects arise due to solvation of the enzyme and substrate.^{35, 41, 45,46} Extensive protein solvation by D₂O can result in a pronounced positive shift of redox potentials. ^{19, 47} However, the negative shift in the E⁰′ of DyPB

(Figure S1-D) from -292 mV in H₂O to -305 mV in D₂O suggested that the medium effect is unlikely to contribute to the observed inverse isotope effect of $(k_{cat}/K_M)^{ABTS}$. By process of elimination, it is therefore likely that the strong inverse sKIE is due to the release of water from the heme iron during catalysis. The magnitude of the inverse sKIE can be used to estimate the number of aqua or hydroxo ligands dissociating from the metal center. The fractionation factor, Φ, is ~0.7 per O-H ligand on average and is multiplicative. 48 Dissociation of one, two, and three water molecules will have sKIEs of 0.49 (Φ^2), 0.24 (Φ^4), and 0.12 (Φ^6), respectively. This method has been employed to elucidate kinetic details of several metalloproteins including *El*DyP. ^{19, 49-51} The ${}^{\rm D}(k_{cat}/K_M)^{\rm ABTS}$ of DyPB, 0.13, corresponding to the release of three water molecules, could come from the displaced sixth water ligand in ERS, and the two water molecules produced during Cpd I formation and reduction (Scheme 1).

Cpd I formation in DyPB. The intrinsic sKIEs of Cpd I formation of the WT, D153A, and R244L were predicted to be ~1.0 based on their observed sKIEs and viscosity effects (Table 2). Additionally, the intrinsic sKIEs of Cpd I formation should reflect the primary isotope effect from the D₂O₂ and the solvent isotope effect from the D₂O, and their relationship is multiplicative.⁵² As discussed above, a strong inverse sKIE of $(k_{cat}/K_M)^{ABTS}$ implies that displacement of the sixth ligand. H₂O, in ERS by H₂O₂ is important for Cpd I formation, which should result in a theoretical solvent isotope effect of 0.49. This was predicted to lower the observed primary isotope effect from the D₂O₂. Consequently, the value of the intrinsic primary isotope effect was likely much larger than the observed sKIE (\sim 1.0) for the WT, suggesting that deprotonation of Cpd0 (k_3 in Scheme 1) is likely to be rate-limiting for Cpd I formation. However, unlike the ElDyP, where the O-O bond scission is much less important than the deprotonation for Cpd I formation, 19 the O–O bond scission in DyPB (k_5 in Scheme 1) was proposed to contribute to the Cpd I formation significantly. Since the distal arginine in DyPB facilitates the O-O bond scission ¹⁸ and the Cpd0 protonation and deprotonation, substitution of this residue was expected to drastically decrease the rate of Cpd I formation. This is supported by the observation that the second-order rate constant of Cpd I formation in R244L was three orders of magnitude slower than in the WT.

Cpd I reduction in DyPB. We proposed that the Cpd I is reduced by ABTS via two successive 1e⁻-reduction processes, producing first the Cpd II then the ERS*. We further proposed that the first reduction step is slow, preventing accumulation and detection of the Cpd II. 53-56 Several experimental observations support our hypothesis. First, the substrate, ABTS, is a $1e^-$ -reductant: a $2e^-$ -reduction is only possible if at least two ABTS molecules bind to DyPB and donate their electrons simultaneously to the enzyme. Involvement of multiple, catalytically relevant binding sites is often manifested experimentally as cooperativity. 57-59 Such cooperativity has been observed in the binding of ABTS to ElDyP and, indeed, it has been suggested that ABTS reduces Cpd I in ElDyP via a single 2e⁻-reduction step. However, such cooperativity was not observed for the WT DyPB (Figure S2-B). Second, it has been postulated that the mechanism of Cpd I reduction depends on whether a water molecule is bound to the Cpd I.60 A "dry" Cpd I without water bound is more prone to direct 2e⁻-reduction to ERS*, as is the case for *El*DyP.¹⁹ Alternatively, a "wet" Cpd I, characterized by a bound water, is more prone to a 1ereduction pathway. The inverse sKIE of 0.25 for the Cpd I reduction in DyPB, suggests a "wet" form for the intermediate, which is predicted to undergo two successive $1e^-$ -reductions to produce ERS* via Cpd II. Finally, spectral features corresponding to Cpd II were observed in DyPB variants at pH>7.0,²⁵ demonstrating that Cpd II could occur in this enzyme.

Protein conformational change as an RDS for the overall reaction. It was proposed that the RDS of the DyPB-catalyzed reaction is either Cpd I formation, product release, or a protein conformational change. 19, 61-64 Cpd I reduction was eliminated as a candidate for the RDS because the second-order rate constant with ABTS was ~2.1-fold faster than that of the Cpd I formation. Product release is unlikely to be rate-limiting because the k_{cat}^{ABTS} was viscosity-independent. Therefore, the RDS is either the Cpd I formation or a protein conformational change, which might also be the first irreversible step in a catalytic cycle. It is known that k_{cat}/K_M incorporates the rate constants for steps prior to the first irreversible one in a reaction pathway. Thus, if the Cpd I formation was the first irreversible step, ${}^{\rm D}(k_{cat}/K_M)^{{\rm H}_2{\rm O}_2}$ should be close to ${}^{\rm D}(k_{cat}/K_M)^{{\rm ABTS}}$, as they essentially describe the same part of the reaction: the Cpd I formation. However, significant differences were observed for $^{\mathrm{D}}(k_{cat}/K_{M})$, suggesting that Cpd I formation is not the first irreversible step and, therefore, is unlikely to be the RDS for the overall reaction. If the protein conformational change was the first irreversible step, then the $(k_{cat}/K_M)^{H_2O_2}$ and $(k_{cat}/K_M)^{ABTS}$ would reflect different parts of the reaction, resulting in different sKIEs. Indeed, ${}^{\rm D}(k_{cat}/K_M){}^{\rm H_2O_2}$ and ${}^{\rm D}(k_{cat}/K_M){}^{\rm ABTS}$ were determined to be 0.92 and 0.13, respectively, Thus, a change in protein conformation is likely to be rate-limiting for the overall ABTS oxidation reaction. Moreover, this conformational change likely does not involve significant movement of loop on the protein surface, as the k_{cat} values for both H_2O_2 and ABTS were viscosity-independent and $^{D}(k_{cat})$ was close to unity (1.08, Table 1).

Conclusions

Our detailed kinetic studies investigating the catalytic roles of the distal aspartate and arginine in DyPB help reconcile the reported discrepancy in the catalytic importance of these residues in DvPs. Our results establish that both distal residues are indispensable for DyPB, but that the arginine is catalytically more important than the aspartate. The relative importance of distal residues in B-class DyPs is likely a function of their respective distances to the solvent ligand in the resting state enzyme. The sKIEs highlight mechanistic differences between B-class DyPB and *El*DyP. Specifically, while the deprotonation of Cpd 0 is rate-limiting for Cpd I formation in both enzymes, O-O scission plays a more significant role in DyPB than in ElDyP. Our studies have also shown that aquo release is mechanistically important for both DyPB and ElDyP, which is reflected by significant inverse sKIEs of $(k_{cat}/K_M)^{ABTS}$ and corresponds to the release of three water molecules from the heme iron. Interestingly, Cpd I's of DyPB and ElDyPB were proposed in "wet" and "dry" formats, respectively, which in turn would undergo $1e^{-}$ and $2e^{-}$ reduction pathways. This may have catalytic implications in DyPs' activity. The significant inverse sKIEs of both enzymes also suggest that their ratelimiting steps are likely to involve a conformational change, which may be characteristic of B-class DyPs. These mechanistic insights increase our understanding of the molecular determinants of catalysis in DyPs and facilitate engineering of these enzymes for biotechnological applications.

AUTHOR INFORMATION

Corresponding Author

* Ping Li – pli@k-state.edu

Notes

The authors declare no competing financial interest.

ASSOCIATED CONTENT

Supporting Information

The Supporting Information is available free of charge on the ACS Publications website.

Experimental procedures for mutation, protein expression and purification, biochemical characterization, and steady- and transient-state kinetics (PDF)

ACKNOWLEDGMENT

This work was supported by the awards from NSF CHE1807532 and Johnson Cancer Center to P.L. and by Natural Sciences and Engineering Research Council of Canada (NSERC) Discovery Grant 171359 to L.D.E. L.D.E. is a Tier I Canada Research Chair (CRC) in Microbial Catabolism and Biocatalysis.

REFERENCES

- Colpa, D. I.; Fraaije, M. W.; van Bloois, E., DyP-type peroxidases: A promising and versatile class of enzymes. *J. Ind. Microbiol. Biot.* 2014, 41, 1-7.
- (2) Singh, R.; Eltis, L. D., The multihued palette of dye-decolorizing peroxidases. *Arch. Biochem. Biophys.* **2015**, *574*, 56-65.
- (3) Strittmatter, E.; Plattner, D. A.; Piontek, K., Dye-decolorizing peroxidase (DyP). In *Encyclopedia of Inorganic and Bioinorganic Chemistry*, Wiley & Sons: New York, 2014.
- (4) Sugano, Y., DyP-type peroxidases comprise a novel heme peroxidase family. Cell Mol Life Sci. 2009, 66, 1387-1403.
- (5) Ahmad, M.; Roberts, J. N.; Hardiman, E. M.; Singh, R.; Eltis, L. D.; Bugg, T. D. H., Identification of DypB from *Rhodococcus jostii* RHA1 as a lignin peroxidase. *Biochemistry* 2011, 50, 5096-5107.
- (6) Brissos, V.; Tavares, D.; Sousa, A. C.; Robalo, M. P.; Martins, L. O., Engineering a bacterial DyP-type peroxidase for enhanced oxidation of lignin-related phenolics at alkaline pH. ACS Catal. 2017, 7, 3454-3465.
- (7) Brown, M. E.; Chang, M. C. Y., Exploring bacterial lignin degradation. *Curr. Opin. Chem. Biol.* **2014**, *19*, 1-7.
- (8) Bugg, T. D. H.; Ahmad, M.; Hardiman, E. M.; Rahmanpour, R., Pathways for degradation of lignin in bacteria and fungi. *Nat. Prod. Rep.* 2011, 28, 1883-1896.
- (9) Chen, C.; Shrestha, R.; Jia, K.; Gao, P. F.; Geisbrecht, B. V.; Bossmann, S. H.; Shi, J. S.; Li, P., Characterization of dyedecolorizing peroxidase (DyP) from *Thermomonospora curvata* reveals unique catalytic properties of A-type DyPs. *J. Biol. Chem.* 2015, 290, 23447-23463.
- (10) de Gonzalo, G.; Colpa, D. I.; Habib, M. H. M.; Fraaije, M. W., Bacterial enzymes involved in lignin degradation. *J. Biotechnol.* 2016, 236, 110-119.
- (11) Fernandez-Fueyo, E.; Linde, D.; Almendral, D.; Lopez-Lucendo, M. F.; Ruiz-Duenas, F. J.; Martinez, A. T., Description of the first fungal dye-decolorizing peroxidase oxidizing manganese(II). *Appl. Microbiol. Biotechnol.* 2015, 99, 8927-8942.
- (12) Min, K.; Gong, G.; Woo, H. M.; Kim, Y.; Um, Y., A dye-decolorizing peroxidase from *Bacillus subtilis* exhibiting substrate-dependent optimum temperature for dyes and β-ether lignin dimer. *Sci. Rep.* 2015, 5: 8245.
- (13) Rahmanpour, R.; Rea, D.; Jamshidi, S.; Fulop, V.; Bugg, T. D. H., Structure of *Thermobifida fusca* DyP-type peroxidase and

- activity towards Kraft lignin and lignin model compounds. *Arch. Biochem. Biophys.* **2016**, *594*, 54-60.
- (14) Brown, M. E.; Barros, T.; Chang, M. C. Y., Identification and characterization of a multifunctional dye peroxidase from a lignin-reactive bacterium. ACS Chem. Biol. 2012, 7, 2074-2081.
- (15) Yoshida, T.; Sugano, Y., A structural and functional perspective of DyP-type peroxidase family. Arch. Biochem. Biophys. 2015, 574, 49-55.
- (16) Ligaba-Osena, A.; Hankoua, B.; DiMarco, K.; Pace, R.; Crocker, M.; McAtee, J.; Nagachar, N.; Tien, M.; Richard, T. L., Reducing biomass recalcitrance by heterologous expression of a bacterial peroxidase in tobacco (*Nicotiana benthamiana*). Sci. Rep. 2017, 7: 17104.
- (17) Poulos, T. L., Thirty years of heme peroxidase structural biology. *Arch. Biochem. Biophys.* **2010**, *500*, 3-12.
- (18) Poulos, T. L., Heme enzyme structure and function. *Chem. Rev.* **2014**, *114*, 3919-3962.
- (19) Shrestha, R.; Huang, G. C.; Meekins, D. A.; Geisbrecht, B. V.; Li, P., Mechanistic insights into dye-decolorizing peroxidase revealed by solvent isotope and viscosity effects. ACS Catal. 2017, 7, 6352-6364.
- (20) van Bloois, E.; Pazmino, D. E. T.; Winter, R. T.; Fraaije, M. W., A robust and extracellular heme-containing peroxidase from *Thermobifida fusca* as prototype of a bacterial peroxidase superfamily. *Appl. Microbiol. Biot.* 2010, 86, 1419-1430.
- (21) Sugano, Y.; Muramatsu, R.; Ichiyanagi, A.; Sato, T.; Shoda, M., DyP, a unique dye-decolorizing peroxidase, represents a novel heme peroxidase family. J. Biol. Chem. 2007, 282, 36652-36658.
- (22) Uchida, T.; Sasaki, M.; Tanaka, Y.; Ishimorit, K., A dye-decolorizing peroxidase from *Vibrio cholerae*. *Biochemistry* 2015, 54, 6610-6621.
- (23) Mendes, S.; Brissos, V.; Gabriel, A.; Catarino, T.; Turner, D. L.; Todorovic, S.; Martins, L. O., An integrated view of redox and catalytic properties of B-type *Pp*DyP from *Pseudomonas putida* MET94 and its distal variants. *Arch. Biochem. Biophys.* **2015**, *574*, 99-107.
- (24) Mendes, S.; Catarino, T.; Silveira, C.; Todorovic, S.; Martin, L. O., The catalytic mechanism of A-type dye-decolorising peroxidase BsDyP: Neither aspartate nor arginine is individually essential for peroxidase activity. Catal. Sci. Technol. 2015, 5, 5196-5207
- (25) Singh, R.; Grigg, J. C.; Armstrong, Z.; Murphy, M. E. P.; Eltis, L. D., Distal heme pocket residues of B-type dye-decolorizing peroxidase arginine but not aspartate is essential for peroxidase activity. *J. Biol. Chem.* 2012, 287, 10623-10630.
- (26) Liu, X. H.; Du, Q.; Wang, Z.; Zhu, D. Y.; Huang, Y.; Li, N.; Wei, T. D.; Xu, S. J.; Gu, L. C., Crystal structure and biochemical features of EfeB/YcdB from *Escherichia coli* O157: Asp235 plays divergent roles in different enzyme-catalyzed processes. *J. Biol. Chem.* 2011, 286, 14922-14931.
- (27) Pollegioni, L.; Tonin, F.; Rosini, E., Lignin-degrading enzymes. FEBS J. 2015, 282, 1190-1213.
- (28) Wong, D. W. S., Structure and Action Mechanism of ligninolytic enzymes. Appl. Biochem. Biotech. 2009, 157, 174-209.
- (29) Demontellano, P. R. O., Catalytic mechanisms of heme peroxidases. In *Biocatalysis based on heme peroxidases*, Torres, E.; Ayala, M., Eds.; Springer-Verlag: Berlin, 2010; pp 79-107.
- (30) Roberts, J. N.; Singh, R.; Grigg, J. C.; Murphy, M. E. P.; Bugg, T. D. H.; Eltis, L. D., Characterization of dye-decolorizing peroxidases from *Rhodococcus jostii* RHA1. *Biochemistry* 2011, 50, 5108-5119.
- (31) Enzyme kinetics and mechanism. Cook, P. F.; Cleland, W. W., Eds., Garland Science: New York, 2007.
- (32) Farrell, D.; Miranda, E. S.; Webb, H.; Georgi, N.; Crowley, P. B.; McIntosh, L. P.; Nielsen, J. E., Titration_DB: Storage and analysis of NMR-monitored protein pH titration curves. *Proteins* 2010, 78, 843-857.
- (33) Goodwin, D. C.; Yamazaki, I.; Aust, S. D.; Grover, T. A., Determination of rate constants for rapid peroxidase reactions. *Anal. Biochem.* **1995**, *231*, 333-338.

- (34) Krezel, A.; Bal, W., A formula for correlating *pK_a* values determined in D₂O and H₂O. *J. Inorg. Biochem.* **2004,** *98*, 161-166
- (35) Karsten, W. E.; Lai, C. J.; Cook, P. F., Inverse solvent isotope effects in the NAD-Malic enzyme reaction are the result of the viscosity difference between D₂O and H₂O-Implications for solvent isotope effect studies. J. Am. Chem. Soc. 1995, 117, 5914-5918
- (36) Bazelyansky, M.; Robey, E.; Kirsch, J. F., Fractional diffusionlimited component of reactions catalyzed by acetylcholinesterase. *Biochemistry* **1986**, *25*, 125-130.
- (37) Brouwer, A. C.; Kirsch, J. F., Investigation of diffusion-limited rates of chymotrypsin reactions by viscosity variation. *Biochemistry* **1982**, *21*, 1302-1307.
- (38) Pocker, Y.; Janjic, N., Enzyme-kinetics in solvents of increased viscosity–Dynamic aspects of carbonic-anhydrase catalysis. *Biochemistry* **1987**, *26*, 2597-2606.
- (39) Dunford, H. B.; Hewson, W. D.; Steiner, H., Horseradish peroxidase. XXIX. Reactions in water and deuterium-oxide: Cyanide binding, compound I formation, and reactions of compound I and compound II with ferrocyanide. *Can. J. Chem.* 1978, 56, 2844-2852.
- (40) Fitzpatrick, P. F., Combining solvent isotope effects with substrate isotope effects in mechanistic studies of alcohol and amine oxidation by enzymes. *BBA-Proteins Proteom.* **2015**, *1854*, 1746-1755.
- (41) Gadda, G.; Fitzpatrick, P. F., Solvent isotope and viscosity effects on the steady-state kinetics of the flavoprotein nitroalkane oxidase. *FEBS Lett.* **2013**, *587*, 2785-2789.
- (42) Venkatasubban, K. S.; Schowen, R. L., The proton inventory technique. Crit. Rev. Bioch. Mol. 1984, 17, 1-44.
- (43) Linde, D.; Pogni, R.; Canellas, M.; Lucas, F.; Guallar, V.; Baratto, M. C.; Sinicropi, A.; Saez-Jimenez, V.; Coscolin, C.; Romero, A.; Medrano, F. J.; Ruiz-Duenas, F. J.; Martinez, A. T., Catalytic surface radical in dye-decolorizing peroxidase: A computational, spectroscopic and site-directed mutagenesis study. *Biochem J.* 2015, 466, 253-262.
- (44) Pfanzagl, V.; Nys, K.; Bellei, M.; Michlits, H.; Mlynek, G.; Battistuzzi, G.; Djinovic-Carugo, K.; Van Doorslaer, S.; Furtmuller, P. G.; Hofbauer, S.; Obinger, C., Roles of distal aspartate and arginine of B-class dye-decolorizing peroxidase in heterolytic hydrogen peroxide cleavage. J. Biol. Chem. 2018, 293, 14823-14838.
- (45) Grissom, C. B.; Cleland, W. W., Isotope effect studies of chicken liver NADP malic enzyme–Role of the metal ion and viscosity dependence. *Biochemistry* 1988, 27, 2927-2934.
- (46) Raber, M. L.; Freeman, M. F.; Townsend, C. A., Dissection of the stepwise mechanism to β-lactam formation and elucidation of a rate-determining conformational change in β-lactam synthetase. *J. Biol. Chem.* 2009, 284, 207-217.
- (47) Farver, O.; Zhang, J. D.; Chi, Q. J.; Pecht, I.; Ulstrup, J., Deuterium isotope effect on the intramolecular electron transfer in *Pseudomonas aeruginosa* azurin. *Proc. Natl. Acad. Sci. USA* 2001, 98, 4426-4430.
- (48) Enzyme mechanism from isotope effects. Cook, P. F., Eds., CRC Press: Boca Raton, 1991.
- (49) Flagg, S. C.; Giri, N.; Pektas, S.; Maroney, M. J.; Knapp, M. J., Inverse solvent isotope effects demonstrate slow aquo release from hypoxia inducible factor-prolyl hydroxylase (PHD2). *Biochemistry* 2012, 51, 6654-6666.
- (50) Hangasky, J. A.; Saban, E.; Knapp, M. J., Inverse solvent isotope effects arising from substrate triggering in the factor inhibiting hypoxia inducible factor. *Biochemistry* 2013, 52, 1594-1602.
- (51) Liang, A. D.; Wrobel, A. T.; Lippard, S. J., A flexible glutamine regulates the catalytic activity of toluene *o*-xylene monooxygenase. *Biochemistry* **2014**, *53*, 3585-3592.
- (52) Schowen, K. B. J., Solvent hydrogen isotope effects. In *Transition states of biochemical processes*. Gandour R. D., Schowen, R. L. Eds, Plenum Press: New York, 1978, pp 225-283.
- (53) Mayfield, J. A.; Blanc, B.; Rodgers, K. R.; Lukat-Rodgers, G. S.; DuBois, J. L., Peroxidase-type reactions suggest a

- heterolytic/nucleophilic O-O joining mechanism in the hemedependent chlorite dismutase. *Biochemistry* **2013**, *52*, 6982-6994.
- (54) Yu, S. W.; Girotto, S.; Zhao, X. B.; Magliozzo, R. S., Rapid formation of compound II and a tyrosyl radical in the Y229F mutant of *Mycobacterium tuberculosis* catalase-peroxidase disrupts catalase but not peroxidase function. *J. Biol. Chem.* 2003, 278, 44121-44127.
- (55) Savenkova, M. I.; Kuo, J. M.; de Montellano, P. R. O., Improvement of peroxygenase activity by relocation of a catalytic histidine within the active site of horseradish peroxidase. *Biochemistry* 1998, 37, 10828-10836.
- (56) Ma, Z. X.; Williamson, H. R.; Davidson, V. L., Mechanism of protein oxidative damage that is coupled to long-range electron transfer to high-valent haems. *Biochem J* 2016, 473, 1769-1775.
- (57) Proteins: Structure and function. Whitford, D., J., Eds., Wiley & Sons: Hoboken, NJ, 2005.
- (58) Cattoni, D. I.; Chara, O.; Kaufman, S. B.; Flecha, F. L. G., Cooperativity in binding processes: New insights from phenomenological modeling. *Plos One* 2015, 10: e0146043.
- (59) Edelstein, S. J.; Le Novere, N., Cooperativity of allosteric receptors. J. Mol. Biol. 2013, 425, 1424-1432.

- (60) Jones, P., Roles of water in heme peroxidase and catalase mechanisms. J. Biol. Chem. 2001, 276, 13791-13796.
- (61) Lad, L. The catalytic mechanism of ascorbate peroxidase: Probing effects of changes in enzyme and substrate structure. Ph.D. Thesis, University of Leicester, December 2014.
- (62) Marquez, L. A.; Huang, J. T.; Dunford, H. B., Spectral and kinetic studies on the formation of myeloperoxidase compounds I and II–Roles of hydrogen-peroxide and superoxide. *Biochemistry* 1994, 33, 1447-1454.
- (63) Padovani, D.; Hessani, A.; Castillo, F. T.; Liot, G.; Andriamihaja, M.; Lan, A.; Pilati, C.; Blachier, F.; Sen, S.; Galardon, E.; Artaud, I., Sulfheme formation during homocysteine S-oxygenation by catalase in cancers and neurodegenerative diseases. *Nat. Commun.* 2016, 7:13386.
- (64) van Haandel, M. J. H.; Primus, J. L.; Teunis, C.; Boersma, M. G.; Osman, A. M.; Veeger, C.; Rietjens, I. M. C. M., Reversible formation of high-valent-iron-oxo porphyrin intermediates in heme-based catalysis: Revisiting the kinetic model for horseradish peroxidase. *Inorg. Chim. Acta.* 1998, 276, 98-105.

TOC

